SPREAD SPECTRUM OPTICAL SIGNAL PROCESSORS

by

David Casasent and Demetri Psaltis
Carnegie-Mellon University
Department of Electrical Engineering
Pittsburgh, PA 15213

ABSTRACT

The features and uses of different optical signal processor architectures for diverse spread spectrum applications are reviewed and several new optical system architectures and applications are described.

1. INTRODUCTION

Spread spectrum (SS) systems are of major concern in diverse applications [1-4]. All SS systems use a transmission bandwidth W that is larger than the bandwidth W_i of the information being transmitted. This technique results in larger output SNR values, allows the system to tolerate lower SNR input data, allows operation with negative transmitted SNR, enables more accurate ranging in radar systems, affords better interference rejection, etc. In Sect. 2, we will briefly review these various SS applications and the different spectrum coding schemes used. Any system in which $W > W_i$ can be classified as a SS system and its processing gain

$$G(dB) = \log (SNR_{out}) - \log (SNR_{in}) \tag{1}$$

can be approximated (in general) by

$$G = W/W_i. \tag{2}$$

From (2), we see that for increased processing gain and system performance, a large transmission bandwidth W is desirable (typical values are 10^8-10^9 Hz). This increased signal bandwidth results in the use of long and often complex coded waveforms with large time bandwidth products (TBW). The transmission and generation of such signals to the necessary accuracy as well as their efficient on-line processing are issues of concern in any such system. In this paper, we will concentrate on the processing of such long TBW signals by advanced techniques, specifically optical signal processing [5,6]. This appears to be an SS problem area of major concern and the one in which the parallel and real-time features of optical signal processors will have their major impact.

Because of the large number of SS applications and the large variety of optical signal processor architectures, our analysis will consider six different SS optical signal processing systems (Sects. 3-8). In each case, the advantages and disadvantages of the specific system will be noted and the specific SS system applications for which each appears to be most appropriate will be described.

2. SPREAD SPECTRUM SYSTEMS

The various coding techniques used to spread the bandwidth W_i of the information into a larger transmission bandwidth W are summarized in Table 1.

TABLE 1 SPREAD SPECTRUM CODING TECHNIQUES

Coding	W	W_i	G
Direct Sequence (DS)	$2/t_0$	$2/Nt_0$	N = TBW
Frequency Hopping (FH)	$1/t_0$	$1/Nt_0$	N = TBW
Frequency Modulation (FM)	$2\ bt_0$	$1/t_0$	$2bt_0^2$ = TBW
Hybrid	-	-	-

UNCLASSIFIED

SECURITY CLASSIFICATION OF THIS PAGE (When Data Entered)

REPORT DOCUMENTATION PAGE

READ INSTRUCTIONS BEFORE COMPLETING FORM

1. REPORT NUMBER: AFOSR-TR-80-0861
2. GOVT ACCESSION NO.: AD-A089820
3. RECIPIENT'S CATALOG NUMBER:
4. TITLE (and Subtitle): SPREAD SPECTRUM OPTICAL SIGNAL PROCESSORS
5. TYPE OF REPORT & PERIOD COVERED: INTERIM rept.
6. PERFORMING ORG. REPORT NUMBER:
7. AUTHOR(s): David Casasent and Demetri Psaltis
8. CONTRACT OR GRANT NUMBER(s): AFOSR-79-0091
9. PERFORMING ORGANIZATION NAME AND ADDRESS:
   Carnegie-Mellon University
   Dept. of Electrical Engineering
   Pittsburgh, PA 15213
10. PROGRAM ELEMENT, PROJECT, TASK AREA & WORK UNIT NUMBERS: 61102F 2305/B2 B21
11. CONTROLLING OFFICE NAME AND ADDRESS:
    AFOSR/NE
    Bldg. 410
    Bolling AFB, DC 20332
12. REPORT DATE: 1980
13. NUMBER OF PAGES: 10
14. MONITORING AGENCY NAME & ADDRESS (if different from Controlling Office):
15. SECURITY CLASS. (of this report): UNCLASSIFIED
15a. DECLASSIFICATION/DOWNGRADING SCHEDULE:
16. DISTRIBUTION STATEMENT (of this Report)

Approved for public release;
distribution unlimited.

17. DISTRIBUTION STATEMENT (of the abstract entered in Block 20, if different from Report)
18. SUPPLEMENTARY NOTES
19. KEY WORDS (Continue on reverse side if necessary and identify by block number)
20. ABSTRACT (Continue on reverse side if necessary and identify by block number)

The features and uses of different optical signal processor architectures for diverse spread spectrum applications are reviewed and several new optical system architectures and applications are described.

AIR 445

DD FORM 1 JAN 73 1473 EDITION OF 1 NOV 65 IS OBSOLETE

UNCLASSIFIED

In DS coding, a carrier is amplitude modulated by a bipolar sequence of + 1's and - 1's. The code sequence used can be a pseudo-random code, Gold code, maximum length code, etc. In this scheme, the code length is Nt_0 where N is the length of the code and t_0 is the chip length of each bit of the code. To transmit a "1" or "0" in such a coding scheme, the phase of the carrier in each chip of the code is usually varied by $\pm \pi$. In multi-user systems, codes with low cross-correlation properties are used. These DS coding schemes are the most used ones because of the ease of generation of the signals. They appear to offer nearly optimum processing gain for both white noise and discrete jammers (in frequency or time).

In FH coding, the transmitted signal consists of a time sequence of N different frequencies f_n, each of chip duration t_0, and with a frequency step size Δf between frequencies. We consider contiguous FH coding, where $\Delta f = 1/t_0$. This type of coding is best suited for rejection of discrete frequency jammers. Transmission of a "1" or "0" in such a system is possible by use of different methods such as complementary frequencies, etc. FH coding provides the optimum processing gain for discrete jammers but not for white noise.

One of the most familiar and easily generated forms of SS coding is the use of a pulsed chirp or linear frequency modulated (LFM) signal

$$a(t) = \Pi(t/t_0) \cos (\omega_0 t + bt^2), \tag{3}$$

where t_0 is the duration of the LFM, ω_0 is its center frequency, $2bt_0$ is its bandwidth and $1/t_0$ usually corresponds to the information bandwidth. For data transmission, up chirps and down chirps can be used to transmit "1" and "0" databits respectively. However, the major use of such codes appears to be in radar since they are easily compressed and can be easily generated and analyzed. They are also extensively used in hybrid radar coding schemes.

The final general type of SS coding is best classified as hybrid. It includes all combinations of the above techniques, such as: FH on a DS code, FH chirps with changing center frequency, etc. In Table 1, we list the approximate W, W_i and G values for each coding technique. As seen, the TBW (or the number of independent signal samples) is the major parameter of concern in the generation and processing of these SS signals and in determining the performance of a given SS system.

Several specific SS system issues and applications with which we will be concerned are noted in Tables 2 and 3. Often, the exact time of data transmission is not known and thus the receiver must be synchronized to the signal before data processing and encoding are possible. Synchronization is necessary in all SS systems. In general, the receiver must search all possible locations of the received code to obtain synchronization. In such cases, a moving window or time domain correlation is necessary with a large range window. Acousto-optic (AO) signal processors are especially attractive for this purpose [5]. If the SNR of the received signal is large, a preamble code of, moderate TBW and processing gain can be used to enable acquisition of synchronization. Similarly, short SS codes are adequate and large time delay search windows (to obtain full correlation SNR output and processing gain possible) are not essential as they are when the SNR of the received signal is low. Special coding techniques (such as the use of a preamble with periodic portions that are easily synchronized) can be used to shift the receiver towards synchronization. An FH code is an excellent choice for the preamble since it is easily synchronized and compressed [1, page 185]. In low SNR cases, preambles with large TBW and processing gain are necessary and a search over many time delays is necessary to obtain the full processing gain and output correlation SNR of the system.

TABLE 2 SPREAD SPECTRUM ISSUES

Spectrum Analysis
Synchronization
Preamble
Message Decoding
Multi-user
Doppler and Ranging

TABLE 3 SPREAD SPECTRUM APPLICATIONS

Communications (Passive)
  PRF, DOA, Data Decoding
Communications (Active)
  Large and Low SNR
  Secure
  Multi-user
Radar
  Ranging
  Ambiguity Function

Many sources of interference are possible with white noise and discrete jammers being the two most general cases. In multi-user systems, each user employs a different code and the crosstalk between channels introduces one source of interference. Use of code division multiplexing with orthogonal codes can decrease the extent of this problem. In general, a parallel multi-channel processor capable of correlating the received signal with all possible reference ones is necessary unless special system alterations are used.

In passive detector applications, one desires to know when and if an SS system is transmitting. This often involves passive detection of the signal by spectrum analysis to determine the presence of and value of the PRF of the system and other indications that transmission is occurring. Obtaining direction of arrival (DOA) information and decoding of the data represent other aspects of this problem. Such an SS application generally corresponds to a low SNR case. In DS systems using psueodrandom codes, the phase of the carrier is modulated by 180^0 for each transition of the code. Balanced modulation with a suppressed carrier is attractive in such coding because more power can then be used in the signal and because detection of the PRF and hence the presence of the SS transmission is then more difficult. In covert communications, transmission at low energy to prohibit detection is vital. Long TBW codes are common in such applications. We note that any linear code is not secure. For such cases, cryptographically secure codes are used or the data is first cryptographically encoded and then transmitted using a linear SS code [1, page 175].

SS codes are also of use in radar to increase range accuracy. In general, the SNR of the received signal in radar is far lower (-50 dB is not uncommon) than in computer transmission cases (when SS techniques are primarily used to improve the bit error rate). We distinguish the cases of jammer rejection, increased ranging accuracy for mapping radars, and improved target range and Doppler information as several specific instances of the need for SS techniques in radar. Sophisticated waveforms with large TBW are being considered for most advanced and multi-purpose radars [7]. Depending upon the source and receiver used, a Doppler shift may exist between the received and reference signals. Processing of such data for all time delays and Doppler shifts with large TBW codes most clearly dictates the need for the full parallel processing ability of optical systems.

3. SPACE INTEGRATING CORRELATORS

In a summary of optical signal processing systems for SS applications, we will be primarily concerned with correlators that enable synchronization and decoding of the transmitted data. We will also give major emphasis to the use of optical signal processing architectures employing AO cells rather than 2-D spatial light modulators, because of the better reliability and performance of the former items [5,6]. A schematic diagram of the AO space integrating (SI) correlator [8] is shown in Fig. 1. In this system, the received signal g (t) is fed to the AO cell at P_{1a}. The transmission of P_{1a} varies in time and space proportional to $g(t-\tau)$, where $\tau = x/v$, v is the velocity of propagation in the cell, x is the spatial distance across the cell and τ has units of time but corresponds to a spatial distance x. This AO cell at P_{1a} is imaged by L_1 and L_2 onto a mask at P_{1b} with transmittance $h^*(\xi)$. Letting $\tau = \xi$, the light distribution leaving P_{1b} is $g(t-\xi)\,h^*(\xi)$. Lens L_3 forms the FT of this light distribution and as a function of time at $u = x_3 = 0$ in P_3 we obtain the desired correlation of g and h,

$$u_3(t) = \mathcal{F}\,[g(t-\xi)h^*(\xi)]\,\Big|_{u=0}$$

$$= \int g(t-\hat{x})h^*(\hat{x})d\hat{x}$$

$$= g \circledast h, \tag{4}$$

where the integration is performed in space $\hat{x}$ by L_3 and the output correlation appears as a function of time at P_3.

This system is simple and easily fabricated. It is also flexible since the mask at P_{1b} can be multiplexed in the $\hat{y}$ direction to produce a multi-channel SI correlator. Such a system can be used to correlate one received input signal with multiple reference ones (as in a multi-user SS system).

In this case, a cylindrical/spherical lens set is used for L_1 to L_3 (to form the FT horizontally and image vertically) and a linear output detector array in y_3 at P_3 is necessary.

In another version of this system, consider what occurs if a Doppler shift exists between g and h. In this case, the location of the output correlation peak will shift in x_3. If a linear horizontal output detector array in x_3 is used, the time outputs from the different detectors in the x_3 direction represent the sampled cross ambiguity function of g and h. In Fig. 2 we show the output signals obtained from the basic SI correlator of Fig. 1 for an LFM input [10]. Detailed analysis [10] of this output pattern showed that the width of the output correlation was in excellent agreement with the theoretical values. The different outputs shown in Fig. 2 were obtained from detectors located at different x_3 locations in the output plane P_3 of Fig. 1. The full pattern in Fig. 2 is the ambiguity function for the LFM signal used. The amplitudes of the output peaks, and their locations were again found to be in excellent agreement with theory thus verifying the performance and accuracy of such an optical signal processor.

The final version of such a SI correlator that we discuss uses the system of Fig. 1 as the first stage of a 2 stage processor for radar ambiguity function computation [7]. In this case, a pulse burst radar was used. The received signals from successive pulses were fed to the input AO cell at P_{1a} and their correlations with the reference function h appear in time at the output detector in P_3. These time outputs were then recorded on separate lines on a 2-D spatial light modulator in the second stage of this processor and a 1-D vertical FT was performed across this 2-D signal pattern. The system output is again the ambiguity function with range displayed horizontally and Doppler vertically [7].

The advantage of the SI correlator is the large range delay (essentially infinite, limited by the dynamic range and noise of the output detector) that it can search between g and h. The bandwidth of the system is also large (equal to the bandwidth of the AO cell). Although the input TBW is small (equal to the TBW of the AO cell, typically 10^3), the output TBW is large (essentially infinite). The low input TBW is the major disadvantage of this system. In FT applications, the frequency resolution possible is $1/T_A$, where T_A is the aperture time of the AO cell. Such a system is thus most appropriate for use in synchronization and demodulation of low TBW preambles and codes or moreso for chirp and pulse burst radar signal processing applications.

4. TIME INTEGRATING OPTICAL CORRELATORS

A schematic diagram of the classic time integrating (TI) optical signal processor [11] is shown in Fig. 3. In this system, the received signal f(t) is used to time sequentially modulate a light source such as an LED or laser diode at P_1. The output from P_1 is collimated to uniformly illuminate an AO cell at P_2 fed with the reference signal h(t) with transmittance $h(t-\tau) = h(t-\hat{x})$. The light distribution leaving P_2 is thus $f(t)\, h(t-\hat{x})$. In the system of Fig. 3, P_2 is imaged onto a time integrating output detector at P_3 where the output correlation

$$R(\hat{x}) = \int f(t)\, h(t-\hat{x})dt = f \circledast h \qquad (5)$$

appears in space $\hat{x} = x_3$ at P_3 with the integration being performed in time on the output detector and the correlation appearing in space at P_3.

The advantage of this system is the long integration time possible and hence the ability to correlate long TBW codes using real-time transducers with moderate 1-D specifications. The disadvantage of this system is the low range delay possible (equal to the aperture time of the AO cell at P_2). In this system, the range resolution possible is the reciprocal of the bandwidth of the AO cell. Although the input TBW of this system is large (approximately infinite, being limited by the integration time used and this is a function of the dynamic range and noise of the detector), the output SBW is low (approximately 1000) and equal to the TBW of the AO cell or the SBW of the output detector. It is this latter feature that determines the range resolution ΔR (equal to the reciprocal of the bandwidth of the AO cell) and the maximum range delay R_{max} (T_A, the aperture time of the AO cell). The processing gain of this system is still large (10^6). The major application of this optical signal processor for SS applications appears to be in the correlation of large TBW codes and in certain passive applications in which short range delays are expected (so that a synchronization search over a large range delay is not necessary).

5. 2-D SPACE INTEGRATING FT AND CORRELATOR SYSTEMS

The prior systems did not use the 2-D processing possible on an optical signal processor. When long duration signals are used with large TBW, the 1-D resolution of conventional correlators are not adequate. In such cases, the frequency plane correlator Fig. 4 can be used with a raster recorded input pattern [12] and a Spann mask [13] at P_3. The FT pattern in this system is a folded spectrum with coarse and fine frequency axes [12]. This large input and output TBW (possible because of the 2-D data formats) is of immense use in the analysis and detection of the presence of SS transmissions and in the synchronization of the data transmitted in such systems. Ampex [14] has recently reported fabrication of a system in which separate segments of the input data are recorded on subsequent lines on a 2-D liquid crystal light valve spatial light modulator using an AO cell and vertical axis deflection addressing scheme. This promises to overcome the addressing problem associated with this system.

The use of such a system to provide synchronization of large TBW signals has also been reported. In this case, a raster recorded input signal is used and a unique Spann mask matched spatial filter is placed at P_2. The output correlation plane pattern at P_3 contains a single peak of light with the full SNR and processing gain of the entire code and its location in P_3 indicates the starting location of the code. In this system, synchronization of a code of length $P = MN$ bits with the full processing gain and output SNR is possible with a mask of spatial dimensions $(2M-1)(2N-1)$. This is far less than the $(MN)^2$ mask resolution that would be required in the equivalent multi-channel correlator. Multi-channel parallel AO cells capable of providing DOA signal information [16] and a system in which the crosscorrelation between two raster recorded signals is used to determine DOA [17] have also been reported.

6. 2-D TIME INTEGRATING CHIRP-Z AND TRIPLE PRODUCT PROCESSORS

The 1-D nature of the AO correlators previously considered is a severe limitation in many instances. In Fig. 5, we show the AO version [18] of an optical system that produces a 2-D output using the chirp-Z [19,20] and triple product processor algorithms [21]. Other versions of these systems exist [22,23], however we will concentrate the present discussion on the system topology [18] shown in Fig. 5.

We first consider realization of the FT operation using the chirp-Z algorithm. We write the FT of f(t) as

$$F(\omega) = \int f(t) \exp(-j\omega t)dt. \tag{6}$$

Using the substitution

$$-\omega t = (t-\omega)^2 - \omega^2/2 - t^2/2 \tag{7}$$

in (6), we can rewrite (6) as

$$\begin{aligned} F(\omega) &= e^{-j\omega^2/2} \int f(t)\, e^{-jt^2/2} e^{j(t-\omega)^2/2} dt \\ &= e^{-j\omega^2/2} [f(t)\, e^{-jt^2/2} \circledast e^{jt^2/2}]. \end{aligned} \tag{8}$$

From (8), we see that the FT of f(t) can be realized by: (a) multiplying f(t) by a chirp $\exp(-jt^2/2)$, (b) correlation of f(t) $\exp(-jt^2/2)$ with the chirp $\exp(+jt^2/2)$, and (c) postmultiplication by the chirp $\exp(-j\omega^2/2)$. Step (c) is not necessary if only the magnitude of the FT is desired. The FT of f(t) described in (8) can be performed using the TI system of Fig. 3 by feeding f(t) $\exp(-jt^2/2)$ to the input LED and the chirp $\exp(jt^2/2)$ to the AO cell. The desired FT $F(\omega) = F(x)$ thus appears in the space $x = x_3 = \omega$ at P_3. This system thus allows the FT operation to be performed using a convolution system.

We now consider the triple product processor of Fig. 5. If we ignore AO2, the output plane pattern is the 1-D function $s_1 \circledast s_2$ smeared horizontally in the output plane P_4. When AO1 is properly focused onto AO2 and when AO1 and and AO2 are imaged onto the 2-D time integrating output plane

detector at P_4, the output plane pattern can be described by

$$I(\tau_1, \tau_2) = \int s_1(t)\, s_2(t-\tau_1)\, s_3(t-\tau_2)dt. \tag{9}$$

We first consider how this system of Fig. 5 can be used as a 2-D folded spectrum processor [18] for detecting the presence of SS signals. In this case, we describe the signal by f(t), we premultiply it by a chirp and time sequentially modulate the light source at P_1 by $s_1(t) = f(t) \exp(-jt^2/2)$. Chirp signals $\exp(jat^2/2)$ and $\exp(jbt^2/2)$ are fed to AO1 and AO2 as s_2 and s_3 with the period T_y of the s_2 chirp much less than the period T_x of the s_3 chirp and with the output plane integration time equal to T_x. In the period T_x, many of the chirp signals s_2 are integrated. This causes a discrete rather than a continuous spectrum to be produced in $\tau_1 = y$ at P_4. This results in a folded spectrum output display in which τ_1 is the coarse frequency axis and τ_2 is the fine frequency axis. The fine frequency resolution in $\hat{x} = \tau_2$ is $1/T_x$ and the coarse frequency resolution in $\hat{y} = \tau_1$ is $1/T_y$.

If we choose $s_1(t) = f_1(t) \exp(+jt^2/2)$, $s_2(t) = f_2(t)$ and $s_3(t) = \exp(+jt^2/2)$, then the parallel output plane pattern at P_4 is the ambiguity function

$$I(\tau_1, \tau_2) = I(\hat{y}, \hat{x}) = \chi(\tau, \omega)$$

$$= \int_T f_1(t)\, f_2(t-\tau) \exp(-j\omega t)dt. \tag{10}$$

Systems such as the one in Fig. 5 represent one of the most advanced optical signal processing architectures. Its flexibility is one of its primary advantages. It can be used for high resolution wideband spectrum analysis for SS detection and code determination as well as in the production of ambiguity functions necessary in range and Doppler radar processing. These features are all achieved with moderate input TBW and large output SBW without the use of any 2-D spatial light modulators.

7. HYBRID TIME AND SPACE INTEGRATING SYSTEMS

A variety of hybrid time and space integrating (TSI) signal processors have recently been described. These systems achieved the large integration time and input TBW of a TI system and the large bandwidth and range delay search range possible in an SI system. One such hybrid TSI system [24] is shown in Fig. 6. We will describe its use in achieving synchronization and demodulation of a large TBW FH SS signal. In the system of Fig. 6, the received signal f(t) is fed to the AO cell at P_1, whose transmittance is $f(t-\tau)$. Its 1-D horizontal FT is incident on P_2, where a mask is placed with apertures at horizontal locations corresponding to the different frequencies f_n in the FH code. The vertical ordering of these slits (or frequencies) in the P_2 mask corresponds to the specific sequence f_k of frequencies used in the FH code. The P_2 mask is imaged vertically and focused horizontally onto a time integrating linear output shift register detector at P_3.

When the first chip enters the AO cell at P_1, its FT occurs at the aperture in the top row of the mask at P_2 and this is imaged onto the top detector in plane P_3. The clock rate of the output detector's shift register is $1/t_0$. Thus, as the second chip enters the AO cell, light passes through the aperture in the second row of the P_2 mask. This is imaged onto the second output detector at P_3 where it is added to the prior contents of the first detector (which has now been shifted down by one detector element). This process continues and after N pulses, the output of the detector in P_3 is a correlation peak with the SNR of the full FH code and occurring at a time that indicates when the received signal occurs. Thus, this hybrid time and space integrating correlator achieves the large time delay search possible with SI systems and the large bandwidth of the AO cell and the correlation of a large TBW product signal.

8. SPACE VARIANT SS PROCESSORS

The newest and most advanced types of SS optical signal processors [25-26] use a transmitted code that is nonlinearly coordinate transformed, thus spreading its spectrum. Since the carrier as well as the envelope of the signal is coordinate transformed, the presence of the transmission is not easily detected. Upon reception, the received signal is fed to the AO cell at P_1 of Fig. 7 and the inverse coordinate transform desired is produced at P_3 by filtering with the mask at P_2 as described

elsewhere [10, 27]. This inverse coordinate transformed received signal is then correlated with the reference signal in the frequency plane correlator portion (P_3-P_5) of Fig. 7. If the applied coordinate transformation is a log, a Mellin transform results. In this case, the vertical location of the output correlation peak corresponds to the Doppler shift between the received and reference signal, whereas the time of occurrence of the output correlation peak is proportional to the range delay in the received signal.

Such a 1-D processor can thus be used to provide synchronization of a received signal, demodulation of it, and determination of range and Doppler delays. Of more concern in the use of such nonlinear space-variant processing techniques for spread spectrum is the increased processing gain such systems appear to offer [25].

9. SUMMARY AND CONCLUSION

This brief review and summary of optical signal processing techniques for spread spectrum applications has indicated that a wealth of diverse optical signal processing system architectures exist and that they are appropriate to many of the various aspects and applications of spread spectrum transmission in communications and radar.

10. ACKNOWLEDGEMENT

The support of the National Science Foundation, the Air Force Office of Scientific Research, the Office of Naval Research and motivation by Hanscom Air Force Base for various phases and aspects of the CMU spread spectrum work reported upon is gratefully acknowledged.

REFERENCES

1. R. C. Dixon, Spread Spectrum Systems, (Wiley, New York, 1976).

2. Spread Spectrum Techniques, IEEE Press, Ed. R. C. Dixon (1976).

3. Image Transmission Via Spread Spectrum Techniques, DARPA Annual Technical Reports (1973-1977).

4. Optical Signal Processing for C^3I, SPIE, 209 (Boston, October 1979).

5. Real-Time Signal Processing, SPIE, 154, (San Diego, 1978); 180 (Washington, D.C., 1979); 185 (Huntsville, 1979).

6. Acousto-Optic, SPIE, Monterey (1979).

7. H. Brown and B. Markevitch, SPIE, 128, 204 (1977).

8. D. Hecht, SPIE, 90, 148 (1976).

9. A. Rihaczek, Principles of High Resolution Radar, McGraw-Hill, NY, (1969).

10. D. Casasent, M. Libby and D. Psaltis, SPIE, 202 (1979).

11. R. Sprague and C. Koliopoulos, Appl. Opt., 15, 89 (1976).

12. C. E. Thomas, Appl. Opt., 5, 1782 (1966).

13. R. Spann, Proc. IEEE, 53, 2137 (1965).

14. J. L. Anderson, et al., SPIE, 180 (1979).

15. D. Casasent and R. Kessler, Opt. Commun., 242 (1976).

16. D. Hecht, SPIE, 90, 148 (1976).

17. W. Rhodes, SPIE, 128, 322 (1977).

18. P. Kellman, IOCC, 91 (1978) and SPIE, 185 (1979).

19. L. Rabiner, et al., BSTJ, 1249 (May 1969).

20. H. J. Whitehouse, et al., MUC-TN 1026 Report (January 1973).

21. J. M. Speiser and H. J. Whitehouse, MUC-TN 1355R (May 1974).

22. T. Turpin, SPIE, 154, 196 (1978).

23. J. Cohen, SPIE, 180 (1979).

24. D. Psaltis and D. Casasent, Opt. Lett., (submitted).

25. D. Casasent and D. Psaltis, Opt. Lett., 4, 18 (1979).

26. D. Psaltis and D. Casasent, Appl. Opt., 18, 1869 (1979).

27. P. Kellman and J.W. Goodman, Appl. Opt., 16, 2609 (1977).

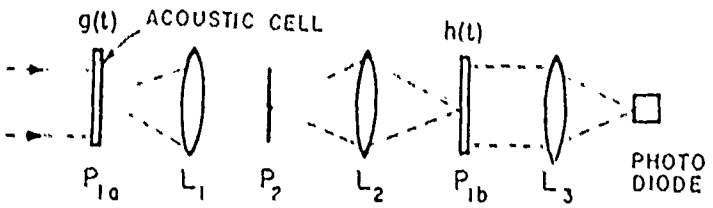

Fig. 1 Schematic diagram of an SI AO optical correlator.

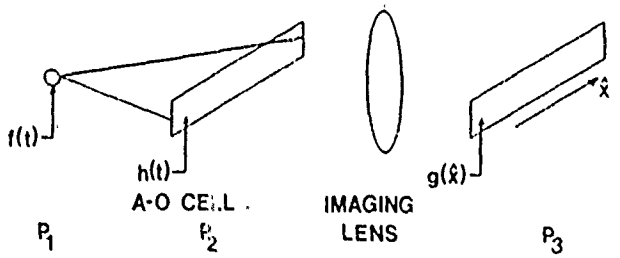

Fig. 3 Schematic diagram of a TI AO optical correlator.

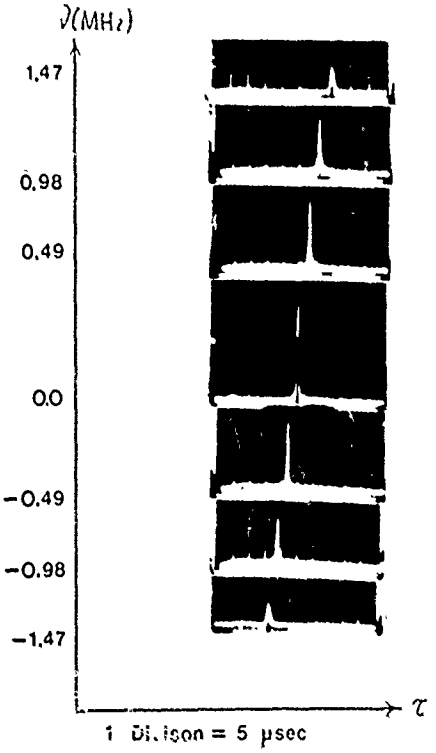

Fig. 2 Representative multi-channel outputs from the TI system of Fig. 1 when used as an ambiguity function processor [10].

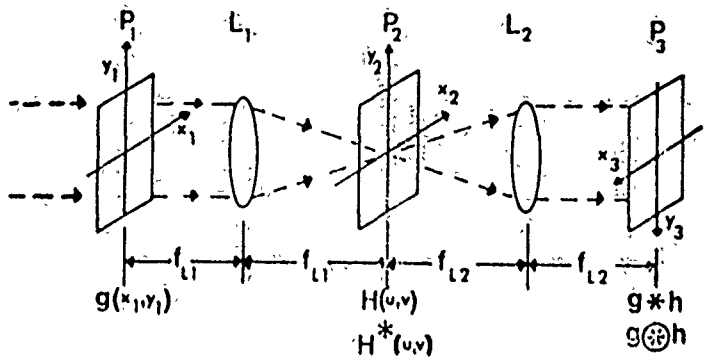

Fig. 4 Schematic diagram of an optical frequency plane correlator or Spann folded spectrum processor.

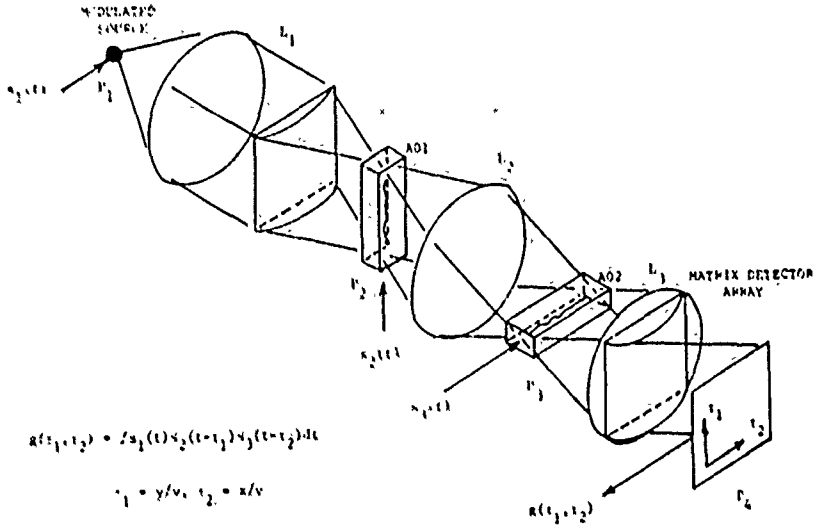

Fig. 5 Schematic diagram of the acousto-optic triple product processor (after [18]).

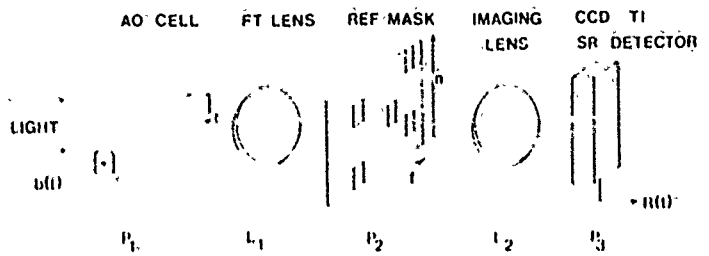

Fig. 6 Hybrid TSI spread spectrum signal processor [24].

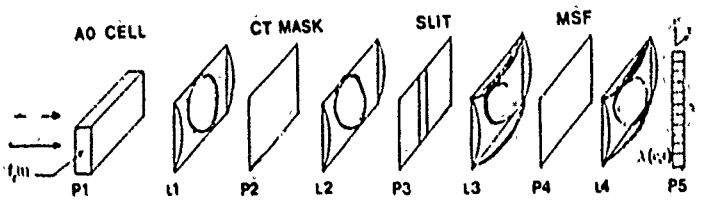

Fig. 7 Space-variant spread spectrum optical signal processor.